

Fast solution of optimal control problems in the selective cooling of steel

F. Tröltzsch and A. Unger
Fakultät für Mathematik
D-09107 Chemnitz

March 9, 1999

Abstract

We consider the problem of cooling milled steel profiles at a maximum rate subject to given bounds on the difference of temperatures in prescribed points of the steel profile. This leads to a nonlinear parabolic control problem with state constraint in a 2D domain. A method of instantaneous control is applied to set up a fast solution technique.

Keywords: Cooling steel, nonlinear heat equation, optimal control, state constraints, instantaneous control, finite element method

AMS subject classification: 49-04,80A20,80A23,90C90,93C20,93C95

1 Introduction

The selective cooling of steel profiles is an important part of the production process in steel mills. Intelligent future strategies aim to combine a reduction of temperature in the rolled profile with an equalization of its interior temperature distribution. An accelerated optimal cooling will reduce the amount of investment in cooling sections. Moreover, it is able to stabilize the interior structure of the steel during phase transitions. Reducing the temperature in the profile as uniformly as possible leads to a higher quality of the steel.

We believe that the intuition of engineers alone is not able to control this process. The mathematical tools of optimal control theory will be helpful to find optimal cooling strategies.

We have reported on this issue in a number of mathematical papers, for instance in Krenzel et.al. [4] and Lezius and Tröltzsch [6], where a method

of feasible direction was developed to solve the optimal control problem. The numerical tests confirmed the stability and reliability of the method. However, the computing time was high.

A very similar problem was discussed by Landl and Engl [5] for a slightly different technical background. In contrast to our setting, where the intensity of cooling of spray nozzles can be chosen continuously, in [5] the intensity is controlled by switching on and off the nozzles.

The rolled steel profiles vary in form and size. Therefore, optimization is needed for a great variety of cases. Corresponding software tools have to deliver the solution in a short time to allow an interactive work of the engineer. A fast solution is also needed for an online-control of the cooling process.

In this paper, we report on a fast numerical method to find good suboptimal cooling strategies. In accordance with [4] and [6], the aim of the process is to reduce the temperature at a maximum rate subject to bounds on the temperature differences occurring in the steel profile. The method presented here is considerably faster than our technique discussed in [4], [6]. We follow an idea of instantaneous control introduced by Hinze and Kunisch [3]. One might expect that this suboptimal strategy is on the expense of accuracy. However, fortunately enough, our suboptimal results exhibit a remarkable coincidence with those obtained in [4].

2 The optimal control problem

A cooling line consists of a certain number of cooling segments, where water is sprayed on the surface of the hot steel profile. Each cooling segment is followed by a zone of air cooling equalizing the developed temperature differences. The basic scheme is shown in Figure 1.

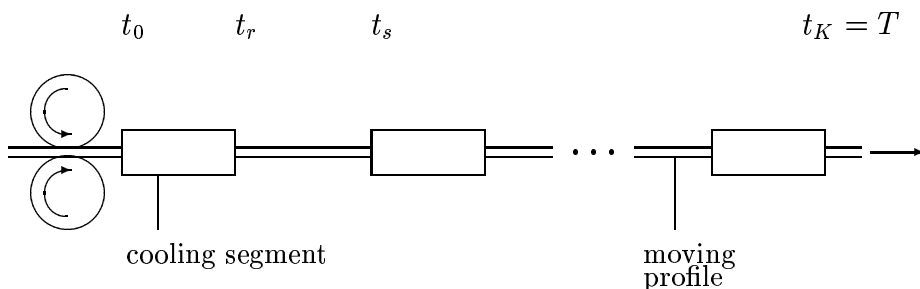


Figure 1: Scheme of a cooling section

In the cooling segments, a certain fixed number of spray nozzles is located in groups around the profile. There can be a sequence of groups in each cooling segment. To explain the mathematical model, let us regard one fixed cross section $\Omega \subset \mathbb{R}^2$ of the steel profile. We follow its run through the whole cooling line. This causes an internal time scheme for the reference domain Ω . The cross section Ω enters the first nozzle group of the first cooling segment at time $t_0 = 0$. Now the surface is sprayed on by the p nozzles of the first nozzle group. After leaving this group, Ω reaches the second one at time t_1 . (Note that there is a small difference to the notation in [4]. In [4], t_1 denotes the time for passing the first cooling segment.) After r steps, Ω has passed the first cooling segment. Now an area of air cooling follows. At time t_s the next cooling segment is entered. Finally, the cross section reaches the end of the last air cooling area at time $t_K = T$, where the profile has passed M zones of water or air cooling.

To shorten the presentation, we rely on the following simplifications: All cooling segments contain the same number r of nozzle groups with the same number p of nozzles. The time for passing any single nozzle group is equal along the whole cooling line. Moreover, the lengths of all cooling segments and air cooling areas are assumed to be equal. Therefore, the time to pass an arbitrary segment is constant. These restrictions are not necessary for the computational technique to work. We adopt them only here to simplify the notation. The resulting discretization of the internal time is given by

$$0 = t_0 < t_1 < \dots < t_r = rt_1 < \dots < t_s = 2t_r < \dots < t_K = Mt_r = T. \quad (1)$$

The heat conduction in axial direction is dominated by the heat exchange in Ω . Moreover, the steel profiles are very long, so that we can view them to be endless. This justifies to neglect the heat conduction in axial direction and to regard a 2D heat equation in our reference domain Ω . Related to this and to the real technical situation, we can assume that the intensity of any single spray nozzle is constant i.e. stationary with respect to the (outer) time.

We associate to each nozzle one part of the boundary $\Gamma = \partial\Omega$ standing for its zone of influence. This leads to a partition of Γ into disjoint subdomains Γ_i , $i = 1, \dots, p$. Denote by u_{ki} the cooling intensity of nozzle i in the group k , $k = 1, \dots, rM$, $i = 1, \dots, p$. Notice that this numbering covers some "phantom" nozzles in the air cooling areas. The numbers u_{ki} will be our *control variables*. In the model we assume that the constraints $0 \leq u_{ki} \leq 1$ are imposed for all k and i . The value 0 stands for an inactive nozzle, while 1 characterizes a nozzle spraying with maximal intensity.

Adopting these notations, the mathematical model for the evolution of the temperature admits the following form, which is equivalent to the model introduced in [4]: The temperature ϑ in the profile is obtained from the nonlinear heat

conduction problem

$$\begin{aligned}
c(\vartheta)\rho(\vartheta) \vartheta_t &= \operatorname{div} (\lambda(\vartheta) \operatorname{grad} \vartheta) && \text{in } Q, \\
\lambda(\vartheta) \partial_n \vartheta &= \sum_{i,k} u_{ki} \chi(\Sigma_{ki}) \alpha(\cdot, \vartheta) (\vartheta_{fl} - \vartheta) && \text{in } \Sigma, \\
\vartheta(0, x) &= \vartheta_0(x) && \text{in } \Omega,
\end{aligned} \tag{2}$$

where $Q = (0, T) \times \Omega$, $\Sigma = (0, T) \times \Gamma$, $\Sigma_{ki} = (t_{k-1}, t_k) \times \Gamma_i$, and $\chi(\Sigma_{ki})$ is the characteristic function of Σ_{ki} . In this setting, ϑ_t and $\partial_n \vartheta$ denote the derivatives $\partial \vartheta / \partial t$ and $\partial \vartheta / \partial n$ with respect to the time and the outer normal n at Γ , respectively. Moreover, the following quantities are used:

- $\vartheta = \vartheta(t, x)$ denotes the temperature at $t \in [0, T]$ and $x \in \Omega$. T stands for the fixed terminal time. Ω is a two-dimensional domain, and ϑ_{fl} is the temperature of the cooling fluid.
- $u_{ki} \in \mathbb{R}$ are the control variables mentioned above. Outside the cooling segments the controls u_{ki} are taken zero to model heat isolation in the areas of air cooling. This is expressed by the characteristic function $\chi(\Sigma_{ki})$ in the boundary condition of (2).
- The coefficients c , ρ , and λ are functions of ϑ denoting heat capacity, specific gravity, and heat conductivity, respectively. The function $\alpha = \alpha(x, \vartheta)$ models the heat exchange coefficient.
- Our cooling process starts with the entrance temperature $\vartheta_0 = \vartheta_0(x)$.

The coefficients c , ρ , λ do not have appropriate properties of smoothness and monotonicity to show the unique solvability of the heat conduction problem. Moreover, the modelling of material changes during the subsequent heating and cooling of the steel is still partially open. The form (2) of the heat equation seems to give only an approximate picture of the temperature changes. Therefore, we do not discuss the question of existence and uniqueness of a solution to (2). Moreover, our computational method will mainly work with linearized versions. For these problems, the existence of a unique solution corresponding to a given vector of controls $u = (u_{ki})$ is clear.

The restrictions on the control variables u_{ki} are given by

$$0 \leq u_{ki} \leq u_k, \tag{3}$$

$k = 1, \dots, rM$, $i = 1, \dots, p$, where $u_k = 0$ for $k = (2j-1)r, \dots, 2jr$ with $j = 1, \dots, M/2$ (air cooling) and $u_k = 1$ otherwise (cooling segment).

The main aim of the cooling process is to reduce the temperature in the domain. Certainly, this can be expressed in various ways. In our model, the

temperature should be reduced in a selection of points $P_n \in \Omega$, $n = 1, \dots, N$, which characterize the hottest regions. In this way, the objective F is defined by the *linear* functional

$$F(\vartheta) = \sum_{n=1}^N a_n \vartheta(T, P_n) \quad (4)$$

with some positive weighting constants a_n .

In the model developed so far, most likely full intensity of all spray nozzles is optimal. However, this strategy is certainly wrong, since very large temperature differences would develop in Ω . This would amount to a low quality of steel and possibly lead to large deformations of the profile. Therefore, we include a finite number of pointwise state constraints in the optimal control problem to bound the temperature differences in Ω . Following [4], these constraints are given by

$$|\vartheta(t, R_\mu) - \vartheta(t, Q_\nu)| \leq \Theta_{\mu\nu}, \quad \mu = 1, \dots, N_R, \quad \nu = 1, \dots, N_Q. \quad (5)$$

In this setting, R_μ and Q_ν denote points from the closure of Ω . For instance, the minimization points $R_\mu := P_\mu$ can be chosen together with some comparison points Q_ν . The situation of our test example is indicated in Figure 2, where the points P_ν and Q_μ are numbered as follows: Q_1 coincides with the origin. Following the boundary of the domain in mathematical positive sense, the next points are $Q_2, \dots, Q_9, P_3, P_2, P_1$. In this way, Q_9 is located at the top, and P_1 is the lowest among the P_i .

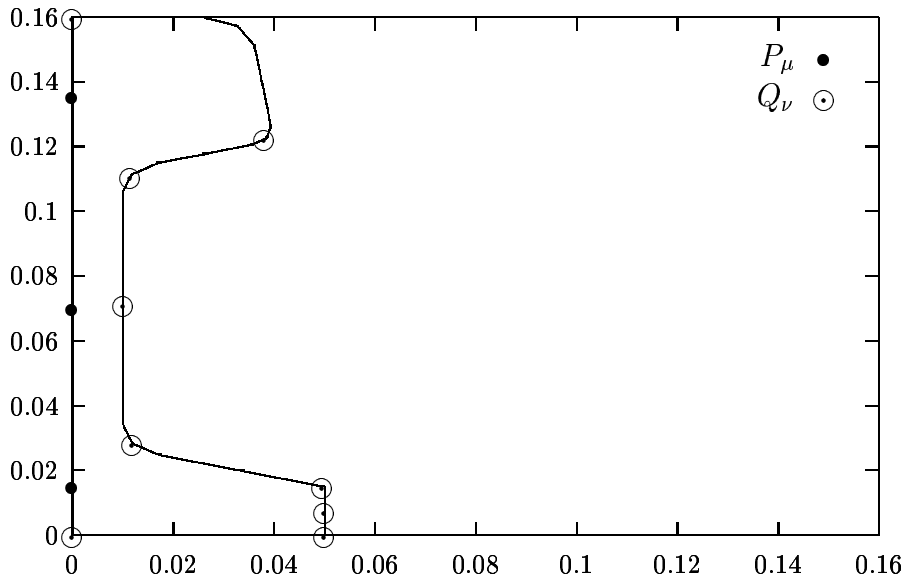


Figure 2: Points of Minimization and of Comparison

Now the definition of the control problem is complete. A more detailed motivation can be found, for instance, in [4], [6]. We refer also to these papers for

details of the numerical solution of the nonlinear parabolic initial–boundary value problem (2) by a finite-element-multigrid method. Moreover, we shall compare our fast optimization technique to obtain suboptimal controls with the more precise method used in these papers. Let us briefly recall for convenience the main ideas characterizing the optimization technique of [4], [6].

3 Iterative solution of the optimal control problem

The optimal control problem is difficult in several respects. The state equation is nonlinear, pointwise constraints on the state are given along with constraints on the controls, and the domain Ω has a curved boundary. Besides the fact that the theory of optimal control problems for nonlinear distributed parameter systems with state-constraints is still far from being complete, the numerical solution is complicated. Readers interested in optimality conditions of first and second order for associated semilinear optimal control problems with state constraints are referred to Casas [1], Raymond and Zidani [8], Goldberg and Tröltzsch [2], and Raymond and Tröltzsch [7].

Solving the heat equation by a sufficiently precise finite element multigrid method, a huge number of state variables appears in the discretized optimal control problem. Due to the use of multiple grids, we are not able to set up a fixed discretized version of the control problem, which might be solved as a finite-dimensional nonlinear optimization problem by available solvers. Moreover, even if we could do so, the size of the problem might exceed the storage capacity.

These remarks have outlined the main difficulties. However, compared with more academic problems discussed in literature, the technical circumstances of the cooling section show an essential advantage: The number of control variables is very low in comparison with the huge number of state variables. Therefore, we decided to use a direct method, where the controls appear as optimization variables, while the state equation is solved only for a certain number of basis controls. In [4], [6] we developed an iterative method of feasible direction. This algorithm proceeds as follows (below, the *control* u stands for the vector (u_{ki}) of control variables):

1. Choose an admissible starting control vector u^0 and compute the associated state ϑ^0 , put $n = 0$. Determine the active state constraints.
2. Linearize the state equation at ϑ^n and u^n , solve it for each standard basis vector of controls. Then the state associated to an arbitrary admissible control can be obtained by superposition.

3. Express the state in the linearized optimal control problem as a linear image of the standard basis vectors using the results of step 2. Solve the associated linear optimization problem with respect to u by the Simplex method. Only active restrictions are considered in the optimization. The result is a new direction of descent \tilde{u} .
4. Put $u^{n+1} = u^n + \gamma(\tilde{u} - u^n)$ and perform a line search with respect to γ while considering all state constraints. Define $n = n + 1$ and go to 2.

This method of feasible direction is of gradient type. Computational tests have shown a quite robust behaviour. We stopped the iteration when the change of the controls was sufficiently small. The convergence rate is quite low. This is the characteristic behaviour of gradient methods. Moreover, the computing time to perform one step of the iteration was very high as well. Notice that in step 2 linear partial differential equations are to be solved for each basis vector. Moreover, we have to solve some nonlinear equations arising from the line search.

On the other hand, the model of heat conduction includes functions which are known only approximately. Especially, the heat exchange function α has to be estimated by a few number of experiments. Recall that we consider the special form of the boundary condition in the heat equation only as a working hypothesis. The whole model contains a number of uncertainties so that it is meaningless to require an extreme accuracy of the optimization technique. It is sufficient to determine a good suboptimal control. The main result of this paper is a very fast and surprisingly exact suboptimal strategy.

4 Suboptimal strategy

In this section we develop the idea of instantaneous control according to Hinze and Kunisch [3] to derive the fast suboptimal solution technique. We apply the following simplifications to accelerate the optimization procedure:

The first simplification is to *linearize the state equation* during certain intervals of time. Nevertheless, the resulting optimal control problem is still nonlinear. The point is the nonlinear coupling of state and control in the boundary condition.

Therefore, we introduce the *heat flux* $v := \lambda \partial_n \vartheta$ on the boundary as a *new control vector*. After having determined the optimal heat flux, we derive an associated original control u by some heuristic formula. Notice that the heat flux has to be nonpositive during a cooling process.

Remark: This approach makes the optimization independent from the working hypothesis on the form of the boundary condition.

Another idea is to *shorten the time horizon* for minimizing the objective func-

tional. This is the core of the instantaneous control technique. In the original formulation of the control problem, we have to achieve the minimal temperature at the final time T . Now we reduce the time horizon to certain small time intervals. The controls associated to the short interval under consideration are chosen to minimize the objective functional at the end of the time interval. In this way, we compute the (sub)optimal solution with respect to a short time horizon regardless of its influence on future times. As a byproduct of linearization, we shall have to solve the state equation only on the associated short time intervals.

Next we shall explain the idea of instantaneous control in more detail. Let $k \in \{1, \dots, K\}$ be one fixed index standing for a nozzle group. The associated time interval $[t_{k-1}, t_k]$ is divided in r_c computational intervals I_{kl} of length $\tau = (t_k - t_{k-1})/r_c$, $I_{kl} = [t_{k-1} + (l-1)\tau, t_{k-1} + l\tau]$, $l = 1, \dots, r_c$. We require constant heat fluxes on I_{kl} and denote them by v_{kli} , $i = 1, \dots, p$. The situation is shown in Figure 3.

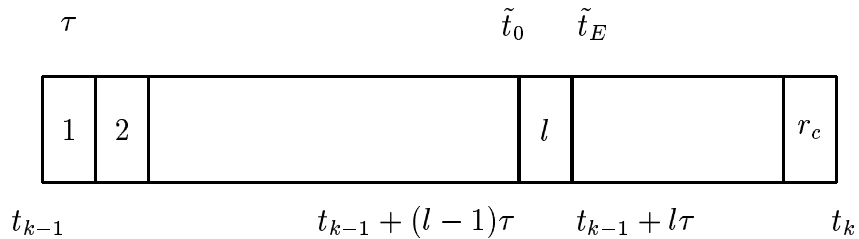


Figure 3: Partition of $[t_{k-1}, t_k]$

Suppose that the optimization process has already been performed for the nozzle groups $1, \dots, k-1$, that is up to the time t_{k-1} . Let $\vartheta_{k-1} := \vartheta(t_{k-1}, x)$ denote the temperature distribution obtained at time t_{k-1} . Freeze the coefficients of the heat equation at ϑ_{k-1} ,

$$c = c(x) := c(\vartheta_{k-1}(x)), \quad \rho = \rho(x) := \rho(\vartheta_{k-1}(x)), \quad \lambda = \lambda(x) := \lambda(\vartheta_{k-1}(x)),$$

on the whole time interval $(t_{k-1}, t_k]$. Here we solve a *finite sequence of linear optimization problems* (P_{kl}) associated to the small subintervals I_{kl} , $l = 1, \dots, r_c$:

Having $k-1$ fixed, regard now the partition of $[t_{k-1}, t_k]$ for $l = 1, \dots, r_c$. Assume that the optimization has already delivered the solution up to the subinterval $I_{k(l-1)}$ and regard the next subinterval I_{kl} . Denote by $\vartheta_{k(l-1)}^I$ the initial temperature computed at the time $\tilde{t}_0 := t_{k-1} + (l-1)\tau$ (we put $\vartheta_{k0} := \vartheta_{k-1}$) and solve the following optimal control problem up to the time $\tilde{t}_E := t_{k-1} + l\tau$:

(\mathbf{P}_{kl}) *Minimize*

$$F(\vartheta(\tilde{t}_E)) = \sum_{n=1}^N a_n \vartheta(\tilde{t}_E, P_n)$$

subject to the state equation

$$\begin{aligned} c(x)\rho(x) \vartheta_t &= \operatorname{div}(\lambda(x) \operatorname{grad} \vartheta) && \text{in } \Omega \\ \lambda(x) \partial_n \vartheta &= \sum_{i=1}^p v_i \chi(\Gamma_i) && \text{on } \Gamma \\ \vartheta(\tilde{t}_0, x) &= \vartheta_{k(l-1)}^I(x) && \text{in } \Omega, \end{aligned} \quad (6)$$

$t \in (\tilde{t}_0, \tilde{t}_E]$, subject to the state constraints

$$|\vartheta(\tilde{t}_E, R_\mu) - \vartheta(\tilde{t}_E, Q_\nu)| \leq \Theta_{\mu\nu}, \quad (7)$$

$\mu = 1, \dots, N_R$, $\nu = 1, \dots, N_Q$, and to the restrictions on the control vector $v = (v_i)$

$$q_{kli} \leq v_i \leq 0.$$

The choice of the bounds q_{kli} will be explained later. Let us consider air cooling areas as cooling segments to unify the notation. Here, the restriction $u_{ki} = 0$ should imply $q_{kli} = 0$. We assume this. Then the only admissible control vector $v = 0$ is optimal in air-cooling areas. We denote the obtained optimal solution by \bar{v}_i , $i = 1, \dots, p$ and put $v_{kli} := \bar{v}_i$, $i = 1, \dots, p$, to keep the index kl underlying the definition of (\mathbf{P}_{kl}).

The solution of the optimal control problems (\mathbf{P}_{kl}) is the core of our suboptimal strategy. However, some further ideas are needed to make this strategy work effectively. The following points are still open: We have to compute the original control vector $u = (u_{ki})$ from the knowledge of the heat fluxes v_{kli} , which served as auxiliary variables. Further, the initial temperatures $\vartheta_{k(l-1)}^I(x)$ must be computed in an appropriate way. In particular, we have to control the error caused by the effects of linearization. The bounds q_{kli} must be chosen.

Remark: The state constraints might be required at further instants of time. We check them only at the times \tilde{t}_E . Owing to this, small violations of the state constraints may occur inside the cooling areas.

(i) Computation of auxiliary controls u_{kli} :

Given the optimal heat fluxes v_{kli} , we define auxiliary controls u_{kli} as follows: Select some computational points $x_i \in \Gamma_i$. Take the mean value of

$$u_{kli}^- = v_{kli} / [\alpha(\vartheta(\tilde{t}_0, x_i))(\vartheta_{fl} - \vartheta(\tilde{t}_0, x_i))]$$

and

$$u_{kli}^+ = v_{kli} / [\alpha(\vartheta(\tilde{t}_E, x_i))(\vartheta_{fl} - \vartheta(\tilde{t}_E, x_i))],$$

that is

$$u_{kli} = \frac{u_{kli}^+ + u_{kli}^-}{2}. \quad (8)$$

(ii) Computation of initial temperatures for $I_{k(l+1)}$:

The initial temperature for the next optimization step can be determined on two ways: Solve the heat equation up to time \tilde{t}_E using the linear or nonlinear equation with boundary conditions of third kind inserting the computed controls u_{kli} . We preferred the nonlinear version. After having determined the auxiliary controls u_{kli} , we solve the *nonlinear* heat conduction problem

$$\begin{aligned} c(\vartheta)\rho(\vartheta) \vartheta_t &= \operatorname{div} (\lambda(\vartheta) \operatorname{grad} \vartheta) && \text{in } \Omega \\ \lambda(\vartheta) \partial_n \vartheta &= \sum_{i=1}^p u_{kli} \chi(\Gamma_i) \alpha(\cdot, \vartheta) (\vartheta_{fl} - \vartheta) && \text{on } \Gamma \\ \vartheta(\tilde{t}_0, x) &= \vartheta_{k(l-1)}^I(x) && \text{in } \Omega \end{aligned} \quad (9)$$

on $[\tilde{t}_0, \tilde{t}_E]$. Then we put $\vartheta_{kl}^I(x) := \vartheta(\tilde{t}_E, x)$. In other words, updating of temperatures is performed nonlinearly, while the optimization is done linearly.

(iii) Choice of the bounds q_{kli} :

The background to define q_{kli} is the relation

$$v_{kli} \approx u_{kli} \alpha(x, \vartheta(t, x)) (\vartheta_{fl} - \vartheta(t, x)).$$

In view of this, inserting the upper bound 1 for u we define

$$q_{kli} = 1 \cdot \alpha(x_i, \vartheta_{k(l-1)}^I(x_i)) (\vartheta_{fl} - \vartheta_{k(l-1)}^I(x_i)) \quad (10)$$

as the lower bound for v_{kli} .

(iv) Definition of original controls:

The optimal control problems (P_{kl}) are solved for $k = 1, \dots, K$ (outer loop) and $l = 1, \dots, r_c$ (inner loop). For each fixed index k , the problems (P_{kl}) deliver the solutions u_{kli} , $l = 1, \dots, r_c$, $i = 1, \dots, p$, on the time intervals I_{kl} . Notice that, according to the given technical construction, only one control vector $u_k = (u_{ki})$ has to be defined on $[t_{k-1}, t_k]$. This is done by the following heuristic formula, which turned out to be very useful:

$$u_{ki} = \frac{\sum_{l=1}^{r_c} l u_{kli}}{\sum_{l=1}^{r_c} l}. \quad (11)$$

This rule reflects that a change in the first small intervals of time can be compensated on the last intervals.

(v) New initial temperature for $[t_k, t_{k+1}]$:

After having solved all subproblems (P_{kl}) , $l = 1, \dots, r_c$, we have determined the suboptimal controls u_{ki} according to (11). Moreover, the final temperature $\vartheta_{kr_c}^I(x)$ was obtained. This is taken as the new initial temperature on $[t_k, t_{k+1}]$, that is $\vartheta_k(x) := \vartheta_{kr_c}^I(x)$.

Alternatively, we might nonlinearly update ϑ on $[t_{k-1}, t_k]$ by solving the *non-linear* heat conduction problem

$$\begin{aligned} c(\vartheta)\rho(\vartheta) \vartheta_t &= \operatorname{div} (\lambda(\vartheta) \operatorname{grad} \vartheta) && \text{in } \Omega \\ \lambda(\vartheta) \partial_n \vartheta &= \sum_{i=1}^p u_{ki} \chi(\Gamma_i) \alpha(\cdot, \vartheta) (\vartheta_{fl} - \vartheta) && \text{on } \Gamma \\ \vartheta(\tilde{t}_0, x) &= \vartheta_{k-1}(x) && \text{in } \Omega, \end{aligned} \quad (12)$$

$t \in [t_{k-1}, t_k]$. Notice that here the control variables are constant on $[t_{k-1}, t_k]$. The the final temperature is taken as the initial temperature for the next interval of time. We did not follow this alternative approach, since it increases the computational effort.

By (i)–(v), the whole interval $[t_{k-1}, t_k]$ is processed. Now we proceed with the next interval $[t_k, t_{k+1}]$. In this way, we arrive after finitely many steps at the final time T . Obviously, this procedure requires the numerical solution of many linear and nonlinear partial differential equations. On using the principle of superposition, we are able to considerably reduce the associated numerical effort. These details are explained in the next section.

5 Numerical implementation

In each nozzle group, the number of controls is very low in comparison with the number of state variables arising from the finite element discretization. In our test example, we have $p = 9$ control variables per nozzle group (there are 16 nozzles in each nozzle group (see Fig. 6), hence, by symmetry, the number of control variables is 9 in each group). In contrast to this, the number of state variables is some thousands. Therefore, in the optimization the state is eliminated by computing the response to each standard basis vector for the control, obtained from the linear equation: Regard, for k fixed, the interval $[t_{k-1}, t_k]$. For all $i = 1, \dots, p$, the *response function* $\vartheta_{ki} = \vartheta_{ki}(t, x)$ is determined by

$$\begin{aligned} c(x)\rho(x) \vartheta_t &= \operatorname{div} (\lambda(x) \operatorname{grad} \vartheta) \\ \lambda(x) \partial_n \vartheta &= \chi(\Gamma_i) \\ \vartheta(0, x) &= 0 \end{aligned}$$

on the interval $[0, \tau]$. These p systems have to be solved only once for the whole interval $[t_{k-1}, t_k]$. On the small subintervals $I_{kl} = (t_{k-1} + (l-1)\tau, t_{k-1} + l\tau)$, the

temperature ϑ is given by superposition,

$$\vartheta(t, x) = \vartheta^I(t, x) + \sum_{i=1}^9 v_i \vartheta_{ki}(t - (l-1)\tau, x).$$

Here, $\vartheta^I(t, x)$ is the fixed part, associated to the initial temperature and homogeneous boundary conditions. It is defined by

$$\begin{aligned} c(x)\rho(x) \vartheta_t &= \operatorname{div} (\lambda(x) \operatorname{grad} \vartheta) \\ \lambda(x) \partial_n \vartheta &= 0 \\ \vartheta(0, x) &= \vartheta_{k(l-1)}^I(x). \end{aligned}$$

The second part represents the contribution associated to the controls v_i . During the optimization process, only the fixed part has to be updated from one subinterval to the next one. Then the optimization problem on (t_{k-1}, t_k) reads

(\mathbf{P}_{kl}) *Minimize*

$$\sum_{n=1}^N \sum_{i=1}^p c_{in} v_i$$

subject to

$$\begin{aligned} \sum_{i=1}^p v_i a_{i\mu\nu} &\leq \Theta_{\mu\nu} - b_{\mu\nu} \\ - \sum_{i=1}^p v_i a_{i\mu\nu} &\leq \Theta_{\mu\nu} + b_{\mu\nu} \\ q_i &\leq v_i \leq 0, \end{aligned}$$

$i = 1, \dots, p$, where

$$\begin{aligned} c_{in} &= c_{kin} = \vartheta_{ki}(\tau, P_n) \\ a_{i\mu\nu} &= a_{ki\mu\nu} = \vartheta_{ki}(\tau, R_\mu) - \vartheta_{ki}(\tau, Q_\nu) \\ b_{\mu\nu} &= b_{kl\mu\nu} = \vartheta^I(t_E, R_\mu) - \vartheta^I(t_E, Q_\mu). \end{aligned}$$

The bounds $q_i = q_{kli}$ are defined according to (10). This linear programming problem is solved by the Simplex method. Its optimal solution $\bar{v} = (\bar{v}_i)$ is denoted by v_{kli} , $i = 1, \dots, p$, to keep the index kl . Notice that the numbers c_{in} , $a_{i\mu\nu}$ have to be computed only once on $[t_{k-1}, t_k]$, while the $b_{\mu\nu}$ and q_i depend on l , hence they must be updated on all subintervals.

During the computations we observed effects of ill-posedness for small values of τ close to the time step for solving the PDEs. This is quite natural: The smaller the time intervals are, the more the associated control variables have to change in order to achieve given changes in the objective. For instance, it was observed that some controls were switching from 0.4 to 1.0 and reverse by changing the discretization of time. To overcome this problem, instead of using the original linear objective functional given above, we minimized the *linearly regularized objective*

$$\operatorname{Min} \quad \sum_{n=1}^N \sum_{i=1}^p c_{in} v_i + \varepsilon \sum_{i=1}^p v_i$$

subject to the constraints given above. This trick stabilized the computed optimal controls.

6 Test example

One of our standard test examples is the cooling of rail profiles. We consider the domain shown in Figure 5 with a low level discretization as in [4], [6].

The concrete formulas for the coefficients c , ρ , λ , α are adopted from these papers. All other data were transmitted by the Mannesmann–Demag–Sack GmbH.

We restrict ourselves to the situation of [4]. That is, we consider 3 minimization points P_n on the axis of symmetry and take them as comparison points too, that is $R_\mu := P_\mu$. 9 points of comparison are chosen on the boundary. Their location is shown in Figure 2. The temperature at these points is compared with the temperature at the minimization points according to the table below.

Point	compared with
P_1	Q_1, Q_2, Q_3, Q_4
P_2	$Q_4, Q_5, Q_6,$
P_3	Q_6, Q_7, Q_8, Q_9

Table 1

In the test example, we regard a cooling line composed of one cooling segment followed by one air cooling area both with length equivalent to 15 seconds. Hence our cross section Ω passes the whole plant in 30 seconds. The cooling segment contains two nozzle groups with 16 spray nozzles each, hence we have 9 control variables (see Fig. 6). This leads to $18 = 2 \cdot 9$ controls acting for 7.5 seconds on different time intervals and on different boundary parts. Following the notation of Section 2 we have $m = 2$, $r = 2$, $p = 9$. This geometry is shown in Figure 4. According to the general setting, for t_1 we get the value 7.5 seconds.

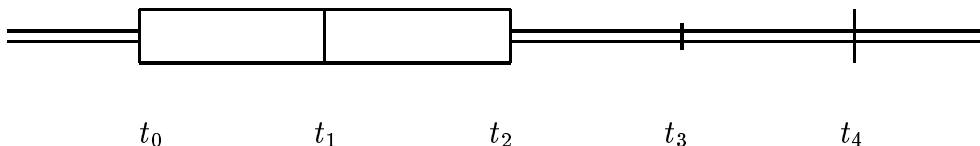


Figure 4: Test geometry

Altogether, this amounts to the following test problem **(E)**:

$$\min F(\vartheta) = \sum_{n=1}^3 a_n \vartheta(T, P_n) \quad (13)$$

subject to

$$\begin{aligned} c(\vartheta)\rho(\vartheta) \vartheta_t &= \operatorname{div} (\lambda(\vartheta) \operatorname{grad} \vartheta) \\ \lambda(\vartheta) \partial_n \vartheta &= \sum_{i,k} u_{ki} \chi(\cdot, \Gamma_i) \alpha(\vartheta)(\vartheta_{fl} - \vartheta) \\ \vartheta(0, x) &= \vartheta_0(x), \end{aligned} \quad (14)$$

to the control constraints

$$0 \leq u_{ki} \leq 1, \quad (15)$$

$k = 1, 2$, $i = 1, \dots, 9$, (cooling segment), $u_{ki} = 0$, $k = 3, 4$, $i = 1, \dots, 9$ (air cooling area), and subject to the state constraints

$$|\vartheta(t, P_\mu) - \vartheta(t, Q_\nu)| \leq \Theta_{\mu\nu}, \quad \mu = 1, \dots, 3, \quad \nu = 1, \dots, 9, \quad (16)$$

where $T = 30$ sec. For Θ we choose the values $\Theta_{\mu\nu} = 8000$ K/m, if the point P_μ is compared with the point Q_ν according to Table 1, and $\Theta_{\mu\nu} = \infty$ otherwise. In the computations we omit the constraints with $\Theta_{\mu\nu} = \infty$. The initial value is chosen as in [4] assuming constant temperatures in 3 areas (see Figure 7). Furthermore, we take the weights $a_1 = a_3 = 3$ and $a_2 = 1$.

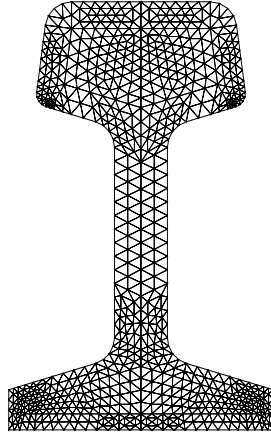


Figure 5: The rail profile

All initial–boundary value problems are solved by a Finite–Element–Multigrid method. In our test runs we worked with a time step of 0.75 seconds to solve the PDE. Therefore, we splitted each nozzle group into 10 parts having just this length $\tau = 0.75$ sec. Obviously, this is the smallest length we can use for computational intervals in our case. In this way, we got the discretization of time $0 = t_0 < t_0 + \tau < \dots < t_0 + 10\tau = t_1 < \dots < t_1 + 10\tau = t_2 < \dots < T$, where $T = 30$ sec and $\tau = 0.75$ sec.

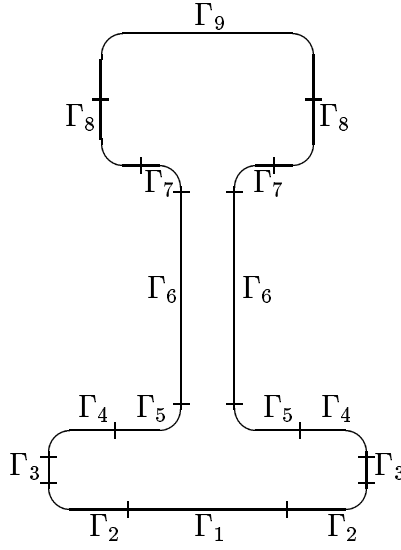


Figure 6: Partition of Γ in the test example

The partition of the boundary Γ into parts Γ_i is roughly indicated in in Figure 6. For the exact geometry of the rail profile we refer to Figure 2.

r_c	1	5	10	Method of [4]
U_{11}	0.3514022539	0.3548936700	0.3573864999	0.3610145792
U_{12}	1.0000000000	0.7982166646	1.0000000000	0.999999049
U_{13}	0.1180339489	0.5883117421	0.4627500743	0.5107195111
U_{14}	1.0000000000	1.0000000000	1.0000000000	0.999999329
U_{15}	1.0000000000	1.0000000000	1.0000000000	0.999999329
U_{16}	0.3364051190	0.3684791893	0.3767291736	0.3832198098
U_{17}	0.5629848913	0.6069457262	0.6123649023	0.6447118269
U_{18}	0.5729147026	0.6618403108	0.6862570122	0.7203573576
U_{19}	0.4343740406	0.4581822405	0.4542159879	0.4888807678
U_{21}	0.3987105180	0.4077419849	0.4134333565	0.4220563562
U_{22}	1.0000000000	0.8962207698	0.9275652482	0.9351645354
U_{23}	0.1143276949	0.0798967829	0.0361622628	0.0770257874
U_{24}	1.0000000000	0.9577281706	0.9777435953	0.9828339652
U_{25}	1.0000000000	1.0000000000	1.0000000000	0.999999636
U_{26}	0.3780443899	0.3878292837	0.3865883499	0.3849542845
U_{27}	0.5813193676	0.5695296293	0.5656343761	0.5785801784
U_{28}	0.5164969503	0.4563890769	0.4494709676	0.4695547182
U_{29}	0.4373472766	0.4294842793	0.4282117893	0.4361204555
$\vartheta(T, P_1)$	781.90893809	781.85488375	781.05464688	780.63044277
$\vartheta(T, P_2)$	755.86971239	752.04789041	751.39936922	750.94385065
$\vartheta(T, P_3)$	854.39305031	853.16742962	853.10581064	851.57897047
$F(\vartheta)$	5664.7756776	5657.1148305	5653.8807418	5647.5720904
CPU	208 sec	106 sec	100 sec	1200 sec / It.

Table 2

By the fast suboptimal strategy, the solution is found in a very short time. The precision of the solution is high, since its distance to the values obtained in [4] is marginal. The only problem appeared through a slight violation of the state constraints of (\mathbf{E}) (see Table 3 below) The computational results for the values 1, 5, 10 for r_c are presented in Table 2. The running time was about 2 minutes on a workstation HP Apollo 9000.

Table 2 contains the computed controls and the corresponding values of the cost functional together with the temperature in the minimization points. Our suboptimal method was applied for different numbers of computational intervals to investigate the effect of their number. The results are compared with those obtained by the algorithm of [4]. We should mention that the slow iterative method of [4] was started at (suboptimal) controls computed by our method for the largest number of computational intervals.

r_c	1	5	10	Method of [4]
$P_1 - Q_1$	-2.56118E+00	-1.63783E+00	-9.67414E-01	-1.13687E-13
- Q_2	-9.58682E+01	-3.75593E+01	-2.26110E+01	-1.29460E+01
- Q_3	-2.43844E+02	-1.31666E+02	-1.50822E+02	-1.38290E+02
- Q_4	-1.11360E+02	-3.15195E+01	-5.07416E+01	-4.24285E+01
$P_2 - Q_4$	-3.79290E+02	-3.01487E+02	-3.21196E+02	-3.13243E+02
- Q_5	-1.81762E+02	-1.83553E+02	-1.84000E+02	-1.84348E+02
- Q_6	-8.08778E+00	-2.50600E+00	-1.09858E+00	-1.11280E-06
$P_3 - Q_6$	-3.38536E+02	-3.30907E+02	-3.28975E+02	-3.27499E+02
- Q_7	-1.53978E+01	-6.99223E+00	-5.90062E+00	-4.31688E-05
- Q_8	-4.69785E+01	-1.87455E+01	-1.09860E+01	-1.24698E-05
- Q_9	-1.27621E+01	-7.16308E+00	-8.09808E+00	-5.97402E-05
$P_1 - Q_1$	-5.66073E+00	-3.55870E+00	-2.11783E+00	-2.07045E-08
- Q_2	-1.07907E+01	-1.66797E+01	-1.33992E+01	-8.75085E-07
- Q_3	-1.10811E+02	-1.02084E+02	-1.04131E+02	-9.02590E+01
- Q_4	-2.17857E+01	-1.23356E+01	-1.35620E+01	-2.37379E+00
$P_2 - Q_4$	-2.80656E+02	-2.74572E+02	-2.76319E+02	-2.65485E+02
- Q_5	-1.66177E+02	-1.69138E+02	-1.69717E+02	-1.70178E+02
- Q_6	-2.05602E+00	+3.01661E-01	+2.02876E-01	-3.41663E-07
$P_3 - Q_6$	-3.15813E+02	-3.10367E+02	-3.09730E+02	-3.09801E+02
- Q_7	-4.28177E+00	-3.52965E+00	-3.74898E+00	-3.18276E-06
- Q_8	-4.20196E+00	-1.18609E+01	-1.10468E+01	-3.55832E-06
- Q_9	-4.15795E+00	-4.06597E+00	-4.75800E+00	-3.43025E-05

Table 3

Table 2 illustrates a surprising precision of the suggested method. Moreover, the last line shows an essential merit: **One** iteration by the method of [4] needs a between five and ten times longer computational time than our whole method. Further, after the first iterations the method of [4] still delivered a solution with considerably larger value than that of our fast approximate solution. To get the

”optimal” values in the last column of the table, the iterative method required 177 iteration steps. Hence we needed 2.5 days to get this slightly better result. Altogether, accuracy and running time of the fast method of instantaneous control are quite convincing. The values also show that computational intervals increase the precision of our method while decreasing the computational time.

However, there appear small problems with the state constraints as shown in Table 3. We list the differences $\vartheta(t_s, P_\mu) - \vartheta(t_s, Q_\nu) - \Theta_{\mu\nu} \text{dist}(P_\mu, Q_\nu)$. The differences indicate satisfied constraints by negative values. Violated constraint have positive values. In other words, the differences measure the level of strict satisfaction of the state constraints. Table 3 shows one violated state constraint measuring the difference of the temperatures in P_2 and Q_6 . The level of violation is low (0.3 °C at most). In our opinion, this is sufficiently small to accept the computed control. Nevertheless, one should carefully observe this problem in more complicated situations.

Finally , we present the plots of the distribution of temperature for the initial and the end time for controls computed with the largest number 10 of computational intervals.

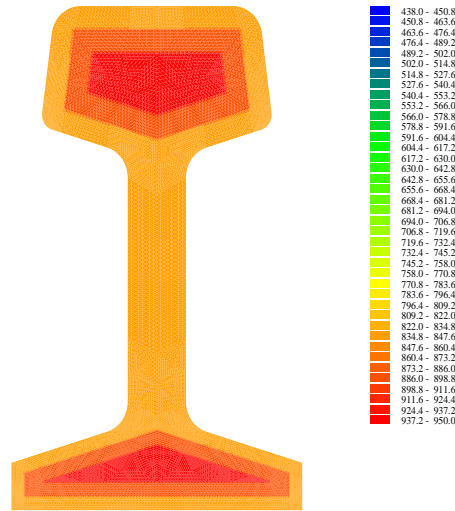


Figure 7: Initial distribution of temperature

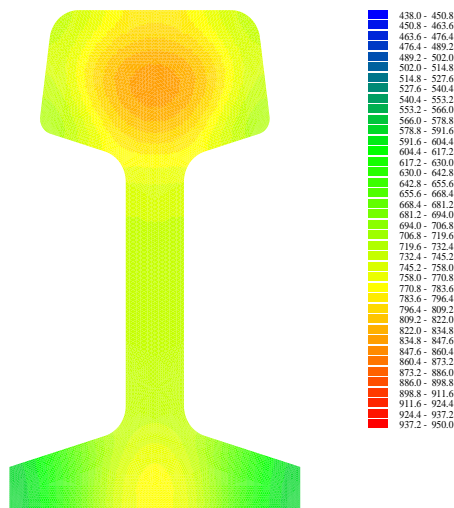


Figure 8: Final temperature distribution

The method presented in the paper should be a useful tool to obtain a first impression on the possibilities of selective cooling. Our experience shows that the computed suboptimal controls are good approximations for the optimal ones. If their accuracy cannot be accepted in some cases, then they will provide at least a very good initial value for the iteration scheme of [4] reducing the associated computing time drastically.

References

- [1] Casas, E.: Pontryagin's principle for state-constrained boundary control problems of semilinear parabolic equations. *SIAM J. Control Optimization* 35 (1997), 1297–1327.
- [2] Goldberg, H. and Tröltzsch, F.: Second order sufficient optimality conditions for a class of non-linear parabolic boundary control problems. *SIAM J. Control Optimization* 31 (1993), 1007–1027.
- [3] Hinze, M., and Kunisch, K.: On suboptimal control strategies for the Navier-Stokes equations. *ESAIM: Proceedings, Vol. 4, 1998, 181–198, Contrôle et Équations aux Dérivées Partielles*, <http://www.emath.fr/proc/Vol.4/>

- [4] Krengel, R., Standke, R., Tröltzsch, F., und Wehage, H.: Mathematisches Modell einer optimal gesteuerten Abkühlung von Profilstählen in Kühlstrecken. *TU Chemnitz, Fakultät für Mathematik*, Preprint 98–6.
- [5] Landl, G., and Engl, H.W.: Optimal strategies for the cooling of steel strips in hot strip mills. *Inverse Problems in Engineering*, 2 (1995), 102–118.
- [6] Lezius, R. and Tröltzsch, F.: Theoretical and Numerical Aspects of Controlled Cooling of Steel Profiles. In: Neunzert, H. (Eds.): *Progress in Industrial Mathematics at ECMI 94*, Wiley-Teubner 1996, 380–388.
- [7] Raymond, J.-P., and Tröltzsch, F.: Second order sufficient optimality conditions for nonlinear parabolic control problems with state constraints. *TU Chemnitz, Fakultät für Mathematik*, Preprint 98–16, to appear.
- [8] Raymond, J.-P., and Zidani, H.: Pontryagin’s principle for state-constrained control problems governed by parabolic equations with unbounded controls, *SIAM Journal on Control and Optimization* 36 (1998), 1853–1879.
- [9] Tröltzsch, F., Lezius, R., Krengel, R. and Wehage, H: Mathematische Behandlung der optimalen Steuerung von Abkühlungsprozessen bei Profilstählen. In *Mathematik– Schlüsseltechnologie für die Zukunft, Verbundprojekte zwischen Universität und Industrie*, K.H. Hoffmann, W. Jäger, T. Lohmann, H. Schunck (Hrsg.), Springer-Verlag 1997, 513–524.